Alexandria Engineering Journal (2022) 61, 13089–13103

HOSTED BY

Alexandria University

Alexandria Engineering Journal

www.elsevier.com/locate/aej
www.sciencedirect.com

Miniaturized 4 × 4 switched-beam Butler Matrix with bandwidth enhancement for 5G communication system

Nazleen Syahira Mohd Suhaimi [a], Nor Muzlifah Mahyuddin [a,*], Widad Ismail [a], Imran Mohd Ibrahim [b]

[a] School of Electrical and Electronic Engineering, Universiti Sains Malaysia, 14300 Penang, Malaysia
[b] Faculty of Electronic and Computer Engineering, Universiti Teknikal Malaysia, 76109 Melaka, Malaysia

Received 10 January 2022; revised 12 April 2022; accepted 4 July 2022

KEYWORDS

Bandwidth enhancement;
Butler Matrix (BM);
Coupler;
Fifth generation (5G) communication system;
Size reduction

Abstract A 4 × 4 Butler Matrix (BM) without phase shifter is proposed to provide bandwidth enhancement and size reduction by removing a conventional 0 dB/90° crossover, two 0° phase shifters and two 45° phase shifters. Two proposed 3 dB/45° patch couplers replace the combination of two conventional 3 dB/90° branch-line couplers and two 45° phase shifters, whilst a modified 0 dB/0° crossover removes two 0° phase shifters from the conventional BM. The −10 dB fractional bandwidths of reflection coefficients and isolations for the proposed BM are 18.46% in simulation and measurement. The −6 dB ± 1.5 dB average transmission coefficient and +45°, −135°, +135° and −45° of output phase differences with 1.8° average phase imbalance are accomplished at 6.5 GHz. The simulated and measured scattering parameters (S-parameters) and phase differences are in close compliance with each other. Four switched-beams pointed at +15°, −50°, +50° and −15° are developed by integrating the proposed BM with inset feeding patch antennas. The proposed BM is miniaturized by 51.56%, whilst the bandwidth performance is enhanced by 9.7% compared to the conventional BM. Hence, this compact BM is a promising candidate for the fifth generation (5G) communication system.

1. Introduction

Wireless communication technology has evolved over the last decades from the first generation (1G) to the fourth generation (4G). However, the expansion of smartphone subscribers and the reflections from tall buildings, plants or other geographical terrains that cause a multipath signal propagation delay

* Corresponding author.
E-mail addresses: nsyahira@student.usm.my (N.S.M. Suhaimi), eemnmuzlifah@usm.my (N.M. Mahyuddin), eewidad@usm.my (W. Ismail), imranibrahim@utem.edu.my (I.M. Ibrahim).

Peer review under responsibility of Faculty of Engineering, Alexandria University.

https://doi.org/10.1016/j.aej.2022.07.014
1110-0168

degrade the quality of the received signal. The 5G communication systems such as multi-access edge.

computing, network function virtualization, massive multi-input multi-output (MIMO), device-to-device communication and massive machine-type communication are expected to cope with better features concerning rapid multi-services to subscribers, higher data rates, better coverage and higher quality of service in the forthcoming decade. Good trade-offs among small device size, low power dissipation, large bandwidth operation and cost-effectiveness become a remarkable challenge for researchers involved in the antenna, radio frequency (RF) and microwave designs to improve channel capacity and large bandwidth. The 6 GHz band (5.9–7.1 GHz) is one of the pioneer 5G candidate spectrum specifications which is suitable for dynamic sharing usage [1]. A large continuous system coverage to the targeted users with higher capacity offered by 5G technology can be achieved using a smart antenna system either switched-beam or adaptive array. Both systems comprise a beamforming network (BFN) with multiple beams pointing in various directions. However, the adaptive antenna array is pricey and has complex designs of the signal processing algorithm and individual RF transceiver chain at the end of each antenna element. Therefore, the BFN

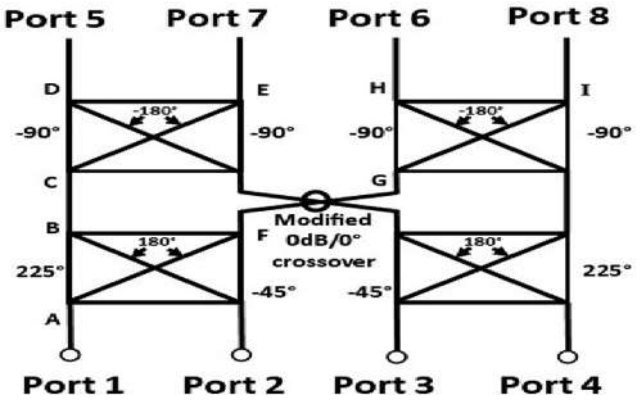

Fig. 2 Signal paths of the proposed 4 × 4 BM.

of the switched-beam antenna system is more attractive to be developed because down-converting the received signal to the baseband is unnecessary.

There are myriad examples of these BFNs such as BM [2,3], Nolen matrix [4,5], Blass matrix [6,7] and Rotman lens [8,9]. The BM becomes more attractive among the other BFNs

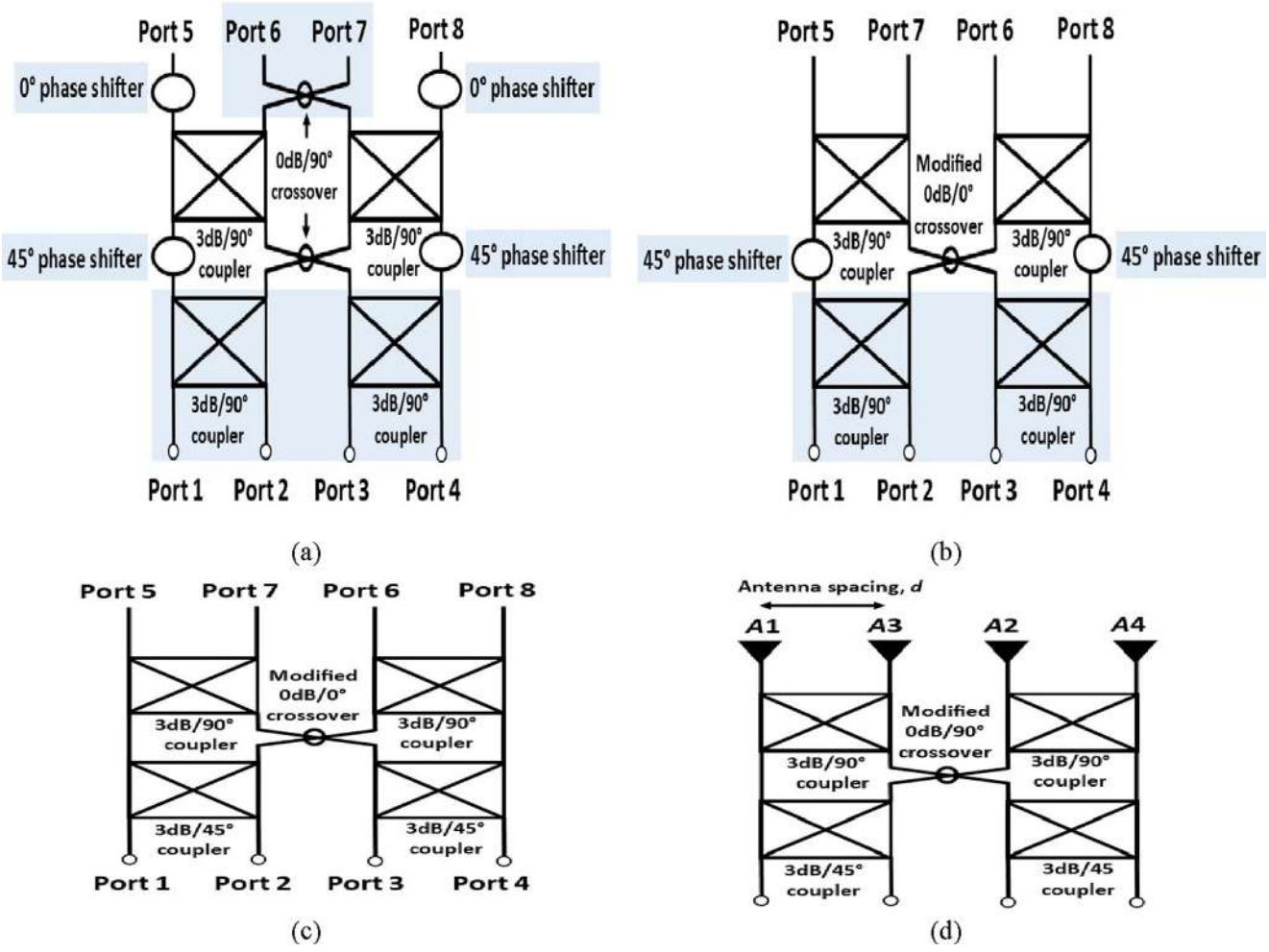

Fig. 1 Block diagram; (a) Conventional 4 × 4 BM. (b) Simplified 4 × 4 BM. (c) Further simplified 4 × 4 BM (proposed). (d) 4 × 4 switched-beam BM (proposed).

Table 1 Phase relation between consecutive output ports of the proposed BM.

		Output ports				Phase differences
		5	6	7	8	
Input ports	1	135°	90°	45°	0°	+45°
	2	90°	−135°	0°	135°	−135°
	3	135°	0°	−135°	90°	+135°
	4	0°	45°	90°	135°	−45°

Table 2 Design specifications of the proposed designs.

	3 dB/90° coupler	3 dB/45° coupler	0 dB/0° crossover	BM
Reflection coefficient and isolation (dB)	≤ −10	≤ −10	≤ −10	≤ −10
Transmission coefficient (dB)	−3 ± 1	−3 ± 1	0 ± 1	−6 ± 3
Output phase difference (°)	90 ± 5	45 ± 5	0 ± 5	+45 ± 5, −135 ± 5, +135 ± 5, −45 ± 5

due to its compact size and low power dissipation [10-13]. Additionally, the BM generates orthogonal beams, which are capable of transmitting and receiving multi-beams concurrently. The BM has N input ports (N beam), N output ports, ($N/2$) log2 (N) hybrid couplers and ($N/2$) log2 (N–1) phase shifters to implement the $N \times N$ BM according to a standard squared number of integers ($N = 2n$). The conventional 4 × 4 BM comprises four 3 dB/90° branch-line couplers, two 0° Schiffman phase shifters, two 45° Schiffman phase shifters and two 0 dB/90° crossovers. However, the circuit size and bandwidth performance of the BM are limited by its coupler and phase shifter. Although the BM can be miniaturized using ridged half-mode substrate integrated waveguide technology [14] and patch structure [15], the bandwidth performances of S-parameters and phase differences are sacrificed. In [16], the BM is miniaturized by stacking the two sides of the substrates and connecting the 45° phase shifters using a via-hole between these layers. Another BM is realized in [17] using switches, lumped couplers and lumped phase shifters which composed of capacitors and inductors. However, low tolerance of the lumped elements in the BM degrade the bandwidth performance. To enhance the bandwidth, the low loss BM using patch element and honeycomb concept on a substrate integrated suspended line platform is reported in [10]. Both coupler and crossover are implemented using patch elements and double-metal layers with a via-hole connection for providing low conductor loss. However, the multi-layer technique in [10] and [18] requires the usage of vias that increase the fabrication difficulties and manufacturing cost.

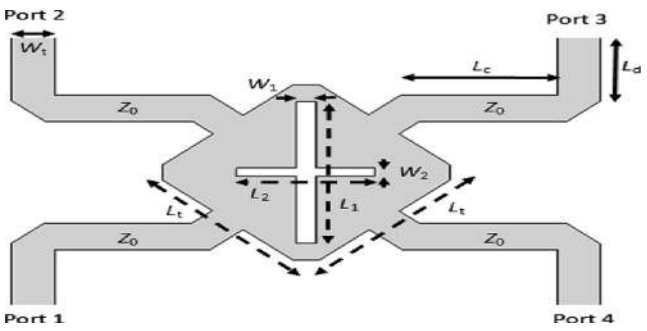

Fig. 3 Physical layout of the optimized 3 dB/90° cross-slotted patch coupler with chamfered edges (Design A).

In the state-of-the-art, the miniaturization of BMs often comes at the price of reduced bandwidth. In this work, the main objective is to develop a single-layered 4 × 4 BM with bandwidth enhancement and size reduction without phase shifter. The miniaturized 4 × 4 BM is realized using two 3 dB/90° cross-sotted patch couplers, two 3 dB/45° cross-sotted patch couplers and a modified 0 dB/0° crossover by eliminating two 0° phase shifters, two 45° phase shifters and a conventional 0 dB/90° crossover, thereby making it remarkably more compact, low power loss and fewer components compared to the conventional design, whilst improving the bandwidth performances. Instead of integrating the 3 dB couplers with 90° output phase differences and 45° phase shifters, employing 3 dB couplers with 45° output phase differences eliminates the use of 45° phase shifters, which contributes to size and loss reduction. The patch topology is adopted from [10], which provides a significant size reduction. The 0 dB crossover is modified to provide 0° output phase difference instead of 90° from the conventional crossover. This modification is realized by extending the lengths of the feeding transmission lines at port 1 and port 2 in the proposed 0 dB crossover design to reduce the output phase difference between port 2 and port 3 from 90° to 0°. The modified 0 dB/0° crossover is capable of eliminating the two 0° Schiffman phase shifters from the conventional BM configuration. The proposed 4 × 4 BM is integrated with inset feeding patch antennas to develop four orthogonal switched-beams. All designs are simulated using CST Microwave Studio software, fabricated onto Rogers RO4003C board with substrate thickness, h of 0.813 mm and dielectric constant, ε_r of 3.38, and measured for verification. The proposed 4 × 4 switched-beam BM can operate between 5.9 GHz and 7.1 GHz with center frequency of 6.5 GHz. The rest of the paper is organized as follows: Section 2 discusses the design methodology of the proposed 4 × 4 switched-beam BM with its components. In Section 3, the per-

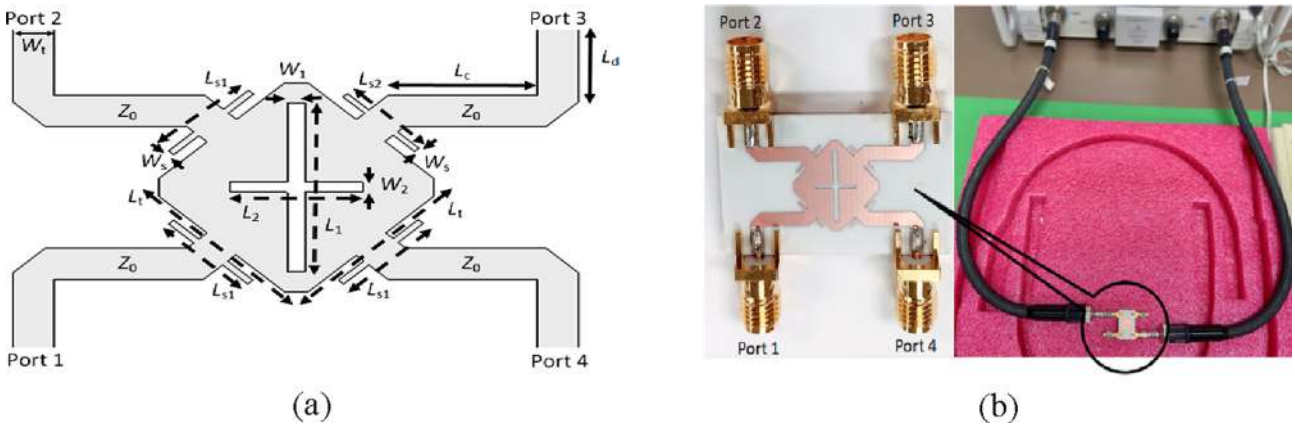

Fig. 4 Proposed 3 dB/90° cross-slotted patch coupler with loaded rectangular stubs (Design B): (a) Physical layout and (b) photograph of the prototype under test.

Table 3 Final dimensions of the cross-slotted patch couplers.

Parameters	Design A	Design B (proposed)
	Values (mm)	Values (mm)
L_t	9.41	9.39
L_1	9.85	9.85
L_2	5.92	5.92
L_c	6.65	6.65
L_d	4.41	4.00
L_{s1}	–	5.00
L_{s2}	–	4.53
W_t	1.84	1.84
W_1	0.80	0.20
W_2	0.60	0.20
W_s	–	0.3

formance results of all proposed designs are presented and discussed. Section 4 presents a comprehensive benchmarking with the contemporary state-of-the-art models. Finally, some concluding remarks are given in Section 5.

2. Design methodology

Fig. 1(a) illustrates a block diagram of the conventional BM which comprises conventional components such as four 3 dB couplers with 90° output phase differences, two 0° phase shifters, two 45° phase shifters and two 0 dB crossovers with 90° output phase differences. The block diagram of the conventional BM is simplified in Fig. 1(b), whereby one conventional 0 dB/90° crossover (top) is removed, whilst port 6 and port 7 are swapped. Meanwhile, two 0° phase shifters are removed, whilst another conventional 0 dB/90° crossover (bottom) is replaced with a modified 0 dB/0° crossover. A further simplification of the BM is proposed as shown in Fig. 1(c), whereby two 45° phase shifters are removed, whilst two conventional 3 dB/90° couplers (bottom) are replaced with two proposed 3 dB/45° patch couplers (bottom). The proposed 4 × 4 BM comprises two proposed 3 dB/90° patch couplers, two proposed 3 dB/45° patch couplers and a modified 0 dB/0° crossover. As depicted in Fig. 1(d), the proposed 4 × 4 BM is integrated with four elements of inset feeding patch antenna to develop four orthogonal switched-beams. In both cases, port 1, port 2, port 3 and port 4 are the input ports where a signal can be excited into the device.

The signal paths of the proposed 4 × 4 BM are denoted in Fig. 2. The input signal goes through A-B-C-D path to port 5 with 135° ($\theta_{51} = \theta_{AB} + \theta_{CD}$) phase shift when port 1 is excited. As the signal goes through the path of A-F-G-H, a 90° ($\theta_{61} = \theta_{AF} + \theta_{GH}$) phase difference is developed between port 1 and port 6. The signal passes through the path of A-B-C-E to support a phase difference of 45° ($\theta_{71} = \theta_{AB} + \theta_{CE}$) between port 1 and port 7. The signal that passes through A-F-G-I path provides a 0° ($\theta_{81} = \theta_{AF} + \theta_{GI}$) phase difference between port 1 and port 8. It can be concluded that the phase shift between the output ports is 45° ($\theta_{51} - \theta_{61} = \theta_{61} - \theta_{71} = \theta_{71} - \theta_{81} = +45°$) when an input signal is excited at port 1. Although the signal is excited on other input ports, the phase differences between the input ports and output ports can be obtained in a similar method. The phase relation between output ports of the proposed 4 × 4 BM is tabulated in Table 1. The phase differences between consecutive output ports are +45°, −135°, +135° and −45° when input port 1, port 2, port 3 and port 4 are driven, respectively. The lengths and widths of the microstrip feeding ports are calculated using microstrip feedline method [19]. The proposed 3 dB/90° patch coupler, 3 dB/45° patch coupler, modified 0 dB/0° crossover and BM are verified with the design specifications given in Table 2.

2.1. Proposed 3 dB/90° cross-slotted patch coupler

The proposed 3 dB/90° cross-slotted patch coupler in this work is a compact design based on the patch structure. The design process of the proposed 3 dB/90° cross-slotted patch coupler is investigated with two steps.

Step 1: Design A; To obtain the equal amplitude of power division (-3 dB) and 90° phase difference between output ports, a pair of asymmetrical cross slots is constructed on the square patch coupler as shown in Fig. 3. The pair of asymmetrical cross slots with unequal lengths (L_1 and L_2) and widths (W_1 and W_2) is developed diagonally on the square patch to perturb the original patch resonator. Moreover, the patch topol-

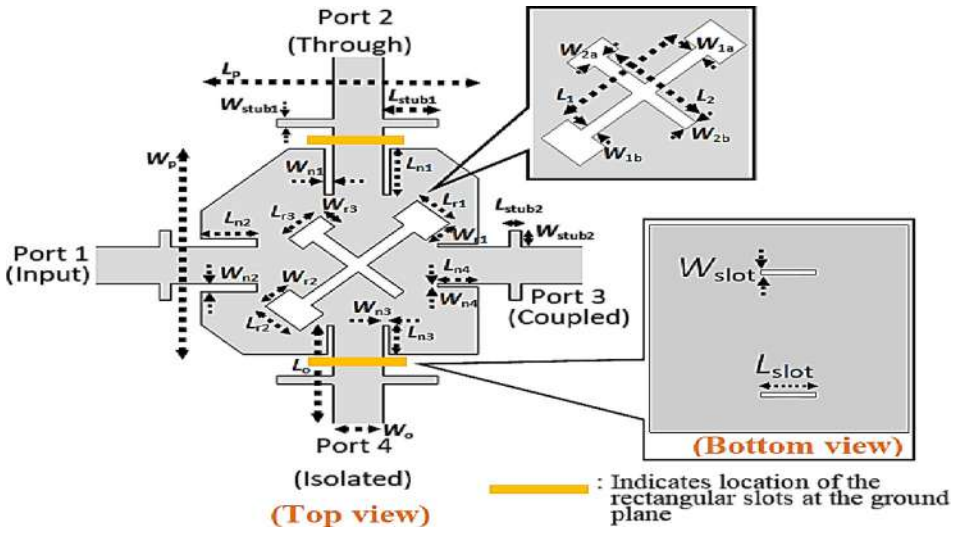

Fig. 5 Physical layout of the proposed 3 dB patch coupler with 45° output phase difference (with ground slot).

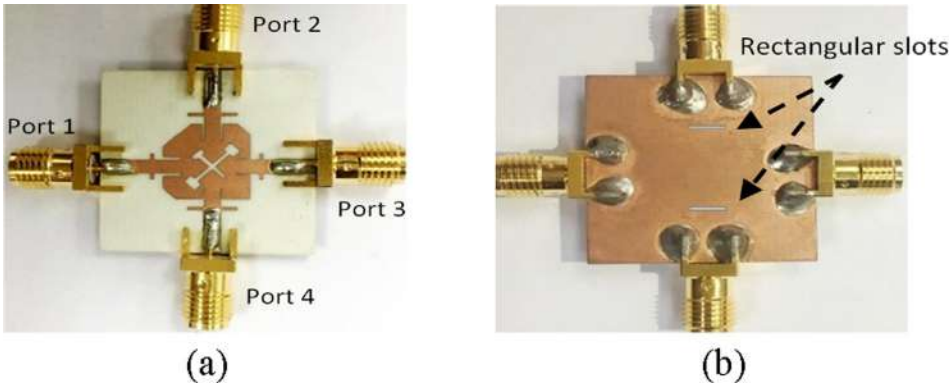

Fig. 6 Photograph of the fabricated proposed 3 dB patch coupler with 45° output phase difference. (a) Top layer. (b) Bottom layer.

Table 4 Optimized parameters of the proposed 3 dB cross-slotted patch coupler with 45° output phase difference.

Parameters	Values (mm)	Parameters	Values (mm)	Parameters	Values (mm)	Parameters	Values (mm)
L_0	7.50	L_{stub2}	0.41	W_{r1}	1.22	W_{stub2}	0.88
L_p	10.12	L_{n1}	2.36	W_{r2}	1.20	W_{n1}	0.29
L_1	5.31	L_{n2}	2.06	W_{r3}	0.73	W_{n2}	0.42
L_2	4.14	L_{n3}	1.48	W_{1a}	0.51	W_{n3}	0.20
L_{r1}	1.65	L_{n4}	1.51	W_{1b}	0.50	W_{n4}	0.20
L_{r2}	1.78	L_{slot}	3.98	W_{2a}	0.59	W_{slot}	0.38
L_{r3}	1.64	W_0	1.84	W_{2b}	0.48		
L_{stub1}	2.02	W_p	10.50	W_{stub1}	0.41		

ogy of this coupler exhibits a smaller circuit size than the conventional 3 dB/90° branch-line coupler. Four feeding ports are placed in the middle of the square patch sides, whilst each feeding port is bent and extended to provide adequate distance between the adjacent ports for the measurement purpose. All ports are matched to a characteristic impedance, Z_o. The dimensions of length, L_t and width, W_t for the microstrip feeding ports can be calculated by substituting the dielectric method [19]. The initial widths of the symmetrical cross slots, W_1 and W_2 are set to 0.2 mm with respect to the available minimum fabrication limit. The physical length of each feeding port is initialized to be a quarter guide wavelength ($\lambda_g/4$), which is equal to L_t and corresponds to the calculated initial value of 7.06 mm. By applying the Pythagorean theorem formula, the initial lengths of the symmetrical cross slots, L_1 and L_2 can be determined. Some parameters of the cross slots such as L_1, L_2, L_t, W_1 and W_2 are optimized to reroute the electric currents around the cross slots. According to the physical limitation of the square patch dimension, L_1 and L_2 are set to be less than $R = 9.98$ mm.

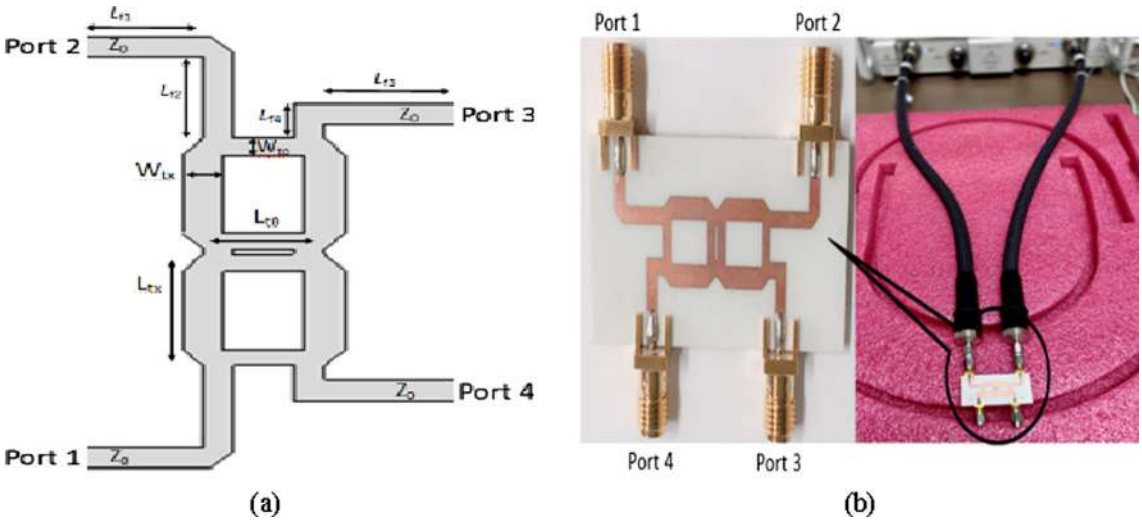

Fig. 7 Modified 0 dB/0° crossover: (a) Physical layout and (b) photograph of the prototype under test.

Table 5 Final dimensions of the modified 0 dB/0° crossover.

Parameters	Values (mm)
L_{to}	7.43
L_{tx}	6.90
L_{f1}	7.52
L_{f2}	7.16
L_{f3}	8.00
L_{f4}	3.09
W_{to}	1.40
W_{tx}	2.50

Each corner of the patch coupler is chamfered to minimize the capacitance and undesired reflections as well as to readjust the microstrip line back to the 50 Ω. Although Design A coupler cannot be described using a closed-form microstrip line theory due to the complicated field distribution of the etched slots, the parameters of the cross slots such as L_1, L_2, L_t, W_1 and W_2 are optimized to reroute the electric currents around the cross slots. The lengths of the asymmetrical cross slots, L_1 and L_2 are set to be less than $R = 9.98$ mm in this case due to the physical limitation of the square patch dimension.

Step 2: Design B (proposed); To enhance the bandwidth performance of S-parameter responses, rectangular stubs are loaded at each feeding port. The lengths of cross slots and stubs are inversely proportional to the frequency of minimum amplitude for the simulated S_{11} and S_{41}. This agrees with a theory which states that the length of any transmission line varies inversely with the frequency of propagation according to Eq. (1) [19]:

$$\text{Frequency} = \frac{\text{velocity through dielectric}}{\text{wavelength}} = \frac{c}{\lambda\sqrt{\varepsilon_r}} \quad (1)$$

where c and ε_r denote the velocity of light and dielectric constant, respectively. The physical layout and photograph of the Design B coupler under test are illustrated in Fig. 4(a) and (b), respectively. The area of the square patch ($L_t \times W_t$) is 0.2 $\lambda_0 \times 0.2$ λ_0. Table 3 compares the final dimensions of the Design A and Design B couplers.

2.2. Proposed 3 dB/45° cross-slotted patch coupler

In order to construct the proposed 3 dB patch coupler with a 45° output phase difference without using 45° phase shifter

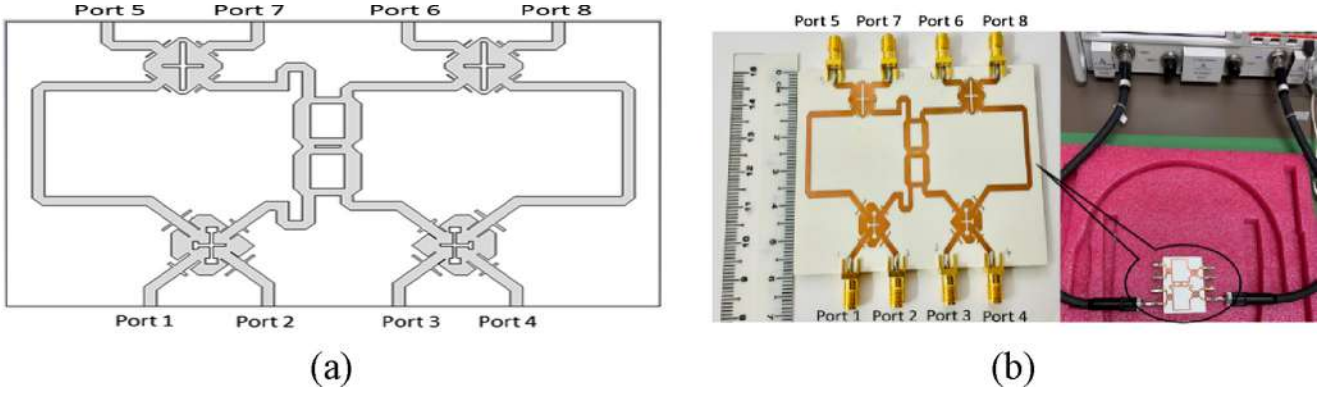

Fig. 8 Proposed 4 × 4 BM: (a) Physical layout and (b) photograph of the prototype under test.

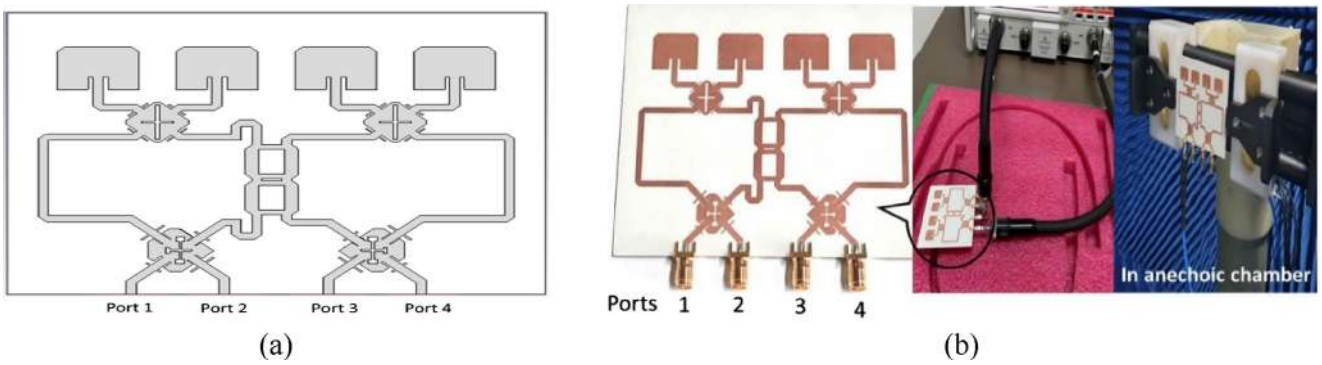

Fig. 9 Proposed 4 × 4 switched-beam BM: (a) Physical layout and (b) photograph of the prototype under test.

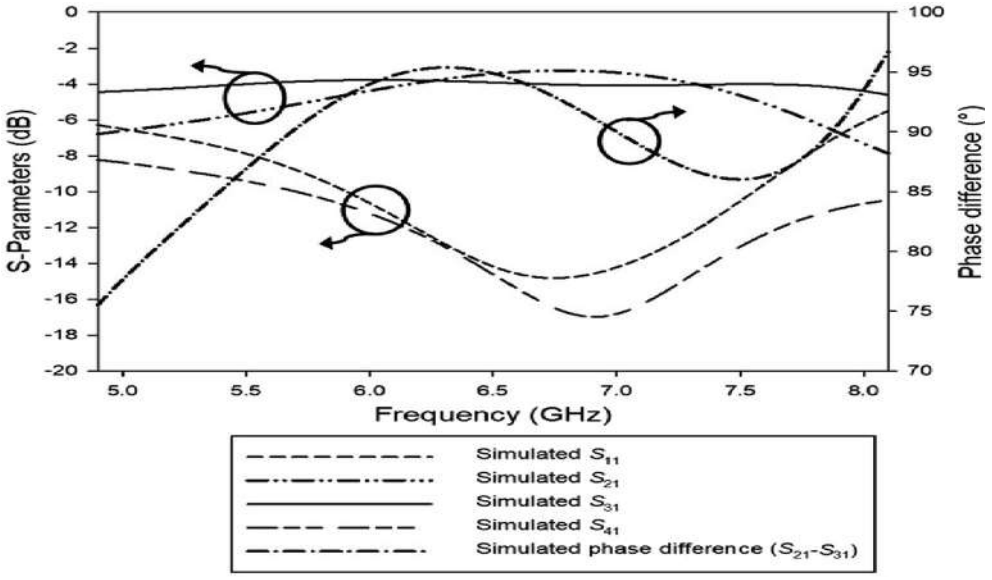

Fig. 10 Simulation results of S-parameters and phase difference for Design A coupler.

while maintaining equal power division (3 dB), the topology design of the proposed 3 dB/90° cross-slotted patch coupler in Fig. 4(a) has been amended by reducing the output phase difference from 90° to 45° through the signal path A-B of the BM as shown in Fig. 2. As the signal is excited at port 1 of this proposed coupler, a 45° output phase difference ($\theta_{45^\circ} = \theta_{AB} - \theta_{AF} = 225^\circ - (-180^\circ)$) is developed. The design steps for obtaining a 3 dB coupling coefficient with 45° output phase difference of the proposed 3 dB/45° cross-slotted patch coupler are done as follows:

I. Dumbbell-shaped slots are loaded at end of the cross slots, whilst the length, L_p and width, W_p of the patch coupler are optimized to ensure a −3 dB coupling coefficient with a compact size.
II. Lengths and widths of the cross slots and rectangular stubs are optimized to reroute the electric currents around the cross slots while maintaining the bandwidth performance of −3 dB coupling coefficient and −10 dB reflection coefficient.
III. Chamfering corners of this coupler are optimized to readjust the impedance matching back to 50 Ω.
IV. Inset feeding technique is adopted by locating notches along each length and width of the patch coupler as a design strategy to accomplish minimum amplitude of S_{11} and S_{41} at the desired resonant frequency of 6.5 GHz.
V. Rectangular ground slots are introduced to further enhance the bandwidth of 45° ± 5° output phase difference without interfering the performance of the −3 dB coupling coefficient.

The physical layout of the proposed 3 dB patch coupler with 45° output phase difference (with ground slot) and the photograph of the fabricated proposed 3 dB patch coupler with 45° output phase difference are illustrated in Figs. 5 and 6, respectively. The optimized parameters of the proposed 3 dB patch coupler with 45° output phase difference are listed in Table 4. The area of the patch ($L_p \times W_p$) is 0.22 λ_0 × 0.23 λ_0 which contributes to a size reduction of 45.72% compared to

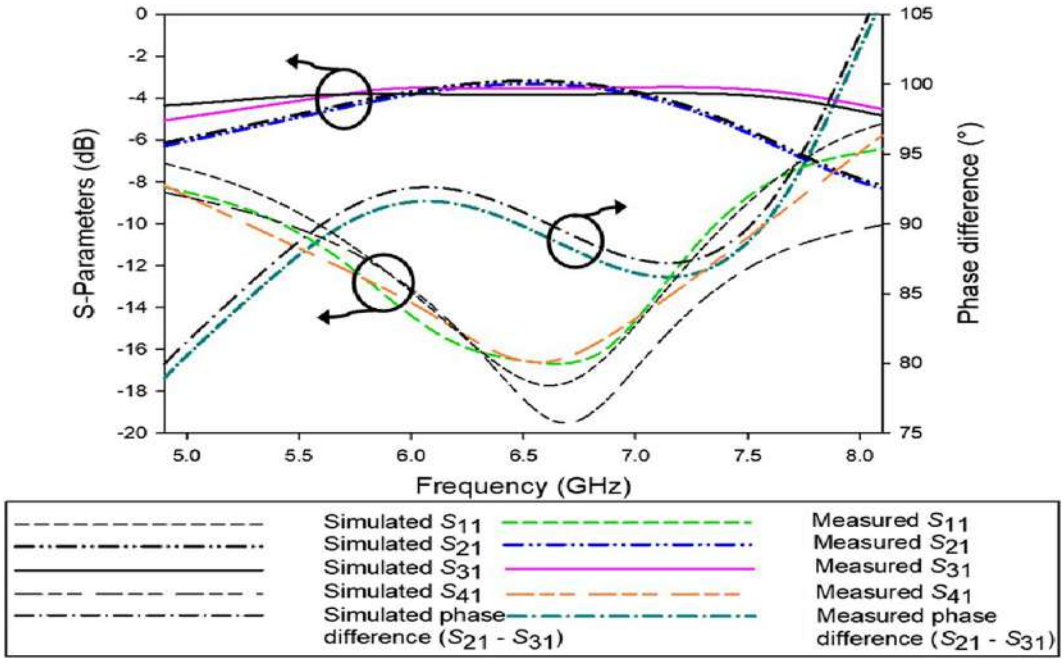

Fig. 11 Simulation and measurement results of S-parameters and phase difference for the proposed 3 dB/90° cross-slotted patch coupler with loaded rectangular stubs (Design B).

the integration of conventional 3 dB branch-line coupler with a 45° Schiffman phase shifter.

2.3. Modified 0 dB/0° crossover

In order to avoid using any additional phase shifter in the proposed 4 × 4 BM, the conventional 0 dB/90° crossover is modified to provide a 0° output phase difference. The 0 dB crossover is constructed by cascading the two conventional 3 dB/90° branch-line couplers. The lengths of the feeding transmission lines at port 1 and port 2 in the proposed 0 dB crossover design are extended to reduce the output phase difference between port 2 and port 3 from 90° to 0° at the center frequency of 6.5 GHz. In addition, the modified 0 dB/0° crossover is capable of eliminating the two 0° Schiffman phase shifters from the conventional BM configuration. The physical layout and fabricated photographs of the modified 0 dB/0° crossover are depicted in Fig. 7(a) and (b), respectively. The final dimensions are listed in Table 5.

2.4. Proposed 4 × 4 BM

The proposed 4 × 4 BM is designed by combining two proposed 3 dB/90° cross-slotted patch couplers, two proposed 3 dB/45° cross-slotted patch couplers and a modified 0 dB/0° crossover. As one crossover (top) is eliminated at the output ports (port 6 and port 7) of the conventional 4 × 4 BM, these ports are swapped to ensure a proper crossing of the output signals. This proposed 4 × 4 BM occupies an area of 1.92 λ_0 × 1.28 λ_0 which contributes to a size reduction of 51.56% compared to the conventional 4 × 4 BM. The physical layout and photograph of the proposed 4 × 4 BM under test are illustrated in Fig. 8(a) and (b), respectively. Each input port (port 1 to port 4) of the proposed 4 × 4 BM is excited accordingly and the signal will be transmitted to each component of the proposed 4 × 4 BM. The BM can provide four sets of consecutive phase outputs based on each input port excitation.

2.5. Proposed 4 × 4 switched-beam BM

The proposed 4 × 4 BM is integrated with four inset feeding patch antennas to investigate the beam steering capability and obtain the radiation patterns. The most suitable value for inter-element spacing between the inset feeding patch antennas in this design is found to be 0.48 λ_0. Fig. 9(a) and (b) show the physical layout and photograph of the proposed 4 × 4 switched-beam BM under test, respectively. Each input port (port 1 to port 4) of the proposed 4 × 4 BM is excited accordingly and the signal will be transmitted to each component of the proposed 4 × 4 BM and passed through the output array elements at port 5 to port 8. Symmetric beam directions with opposite signs are observed when power is excited at port 3 or port 4 compared to the obtained beam directions by exciting port 1 or port 2 due to the symmetric configuration of the proposed switched-beam 4 × 4 BM.

3. Results and discussions

The results from all five proposed circuits are illustrated in Figs. 10–16. The performance results of the proposed 3 dB/90° cross-slotted patch coupler, 3 dB/45° cross-slotted patch coupler and modified 0 dB/0° crossover are explained in Sections 3.1, 3.2 and 3.3, respectively. In Sections 3.4 and 3.5, all simulated and measured results of the proposed 4 × 4 BM and 4 × 4 switched-beam BM are presented and discussed.

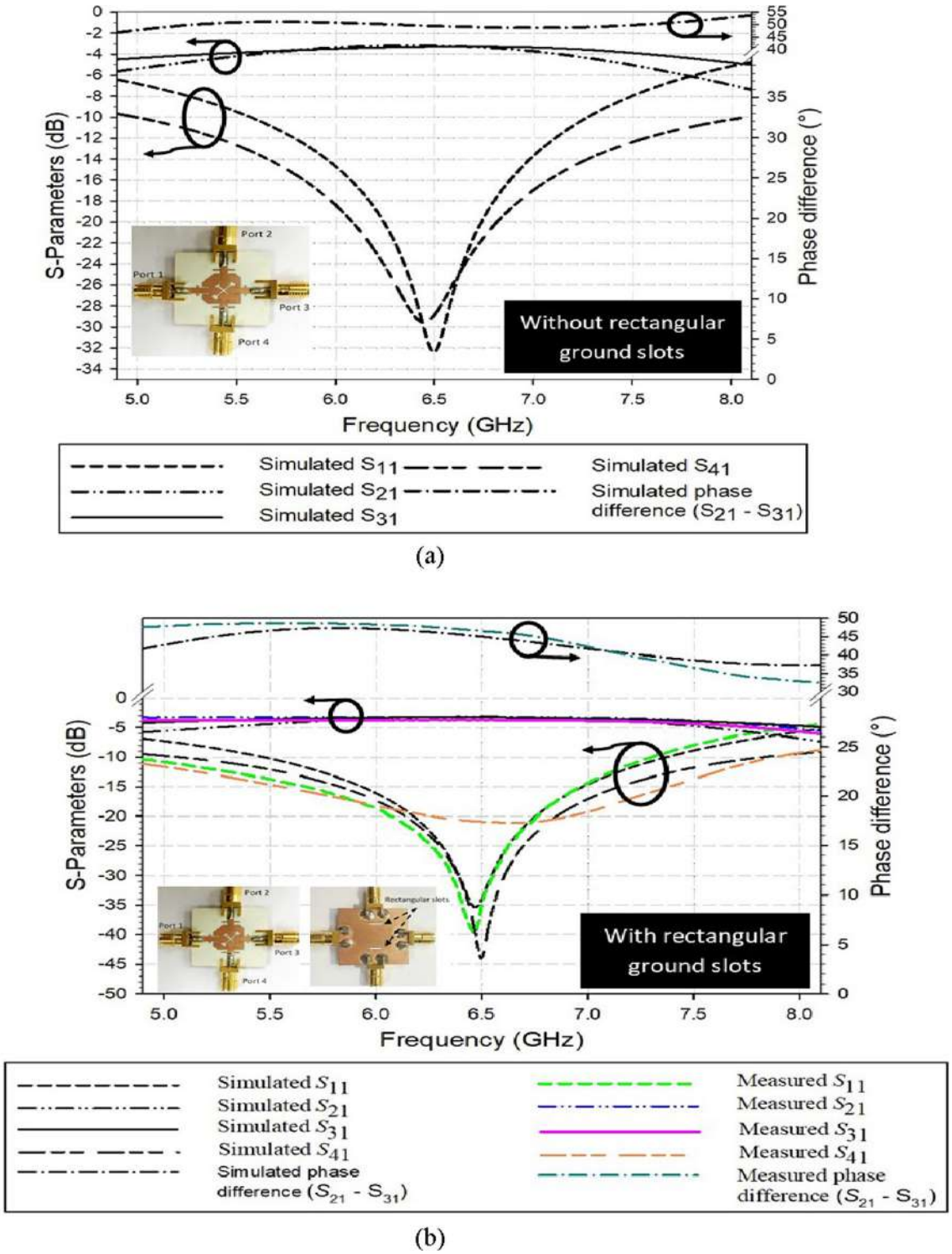

Fig. 12 Performance results of the 3 dB/45° patch coupler. (a) Without rectangular ground slots. (b) With rectangular ground slots (proposed).

3.1. Proposed 3 dB/90° cross-slotted patch coupler

The S-parameter responses of the Design A coupler are simulated as depicted in Fig. 10. As observed in Fig. 10, the −10 dB fractional bandwidth of simulated return loss, S_{11} and isolation, S_{41} for the Design A coupler is 25.38% and 36.76%, respectively. Meanwhile, the bandwidths of 1 dB amplitude imbalance for both simulated transmission coefficient, S_{21} and coupling, S_{31} are 18.31% and 34.61%, individually. The 5° phase imbalance bandwidth of the simulated phase differ-

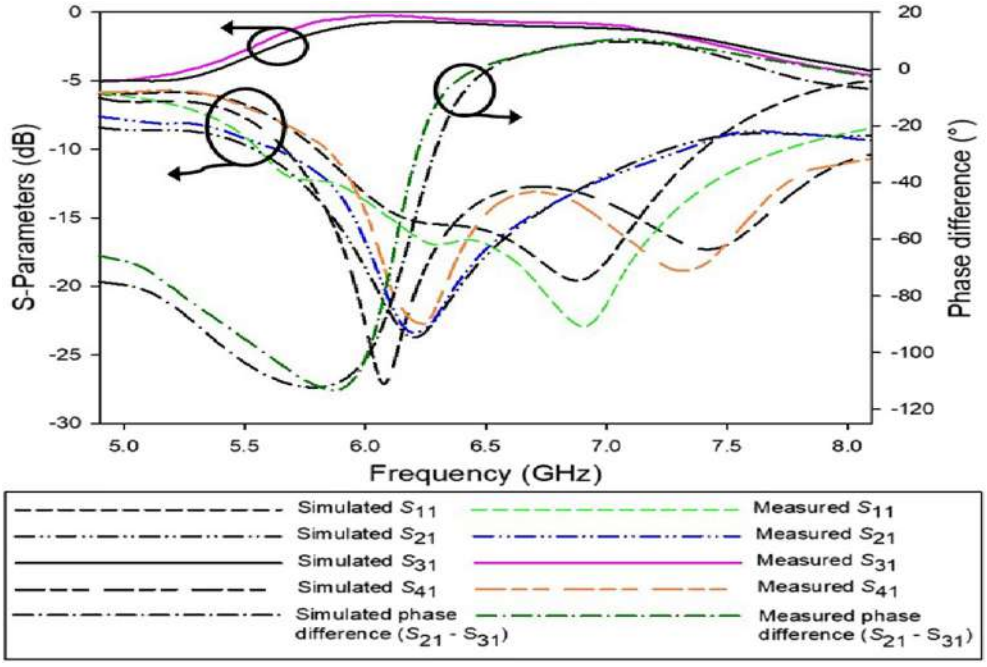

Fig. 13 Performance results of the 0 dB/0° modified crossover under test.

ence between output ports is 40.61%. The bandwidths of S-parameter responses such as S_{11}, S_{21}, S_{31}, and S_{41} in Design A coupler are improved by loading rectangular stubs at each feeding port in Design B coupler.

Fig. 11 depicts the performance results of the proposed 3 dB/90° cross-slotted patch coupler with loaded rectangular stubs (Design B). The −10 dB fractional bandwidths of return loss, S_{11} and isolation, S_{41} for the Design B coupler are 28% and 40.92% in simulation, whilst 30% and 36% in measurement. Meanwhile, the bandwidth of −3 dB ± 1 dB for simulated S_{21} is 19.85%, whilst 36.46% for simulated S_{31}. The bandwidths of 1 dB amplitude imbalance for both measured transmission coefficient, S_{21} and coupling, S_{31} are 34.77% and 18.46%, respectively. The 5° phase imbalance bandwidths of the simulated and measured phase differences between output ports are 37.84% and 38.62%, respectively. The bandwidth enhancement for the proposed 3 dB/90° cross-slotted patch coupler (Design B) is 15.38% compared to the conventional 3 dB branch-line coupler. At 6.5 GHz, the reflection coefficients, S_{11} and isolation, S_{41} are −17.43 dB and −18.37 dB in simulation, whereas −16.41 dB and −16.68 dB in measurement. The simulated transmission coefficient, S_{21} is 3.17 dB, whilst the measured S_{21} is 3.32 dB at 6.5 GHz. Meanwhile, the simulated coupling coefficient, S_{31} is −3.84 dB, whereas the measured coupling coefficient, S_{31} is −3.54 dB. The simulated output phase difference is 90.82° with a phase deviation of 0.82°, whereas the measured phase difference is 89.83° with a phase deviation of 0.17°. A comprehensive comparison between the performance of the proposed 3 dB/90° cross-slotted patch coupler with loaded rectangular stubs (Design B) and the existing patch coupler is shown in Table 6.

3.2. Proposed 3 dB/45° cross-slotted patch coupler

The performance results of the 3 dB/45° patch coupler without rectangular ground slots and with rectangular ground slots are illustrated in Fig. 12(a) and (b). As seen in Fig. 12(a), the −10 dB fractional bandwidths of the simulated S_{11} and S_{41} are 26.02% and 47.07%, accordingly. The 1 dB amplitude fluctuation bandwidth for the simulated S_{21} is 23.69%, whilst 33.90% for the simulated S_{31}. The bandwidth of 5° phase imbalance for the simulated output phase difference is 19.61%. At 6.5 GHz, the simulated S_{11} is –32.37 dB, whereas the simulated S_{41} is −28.86 dB. The simulated S_{21} is −3.17 dB, whereas the simulated S_{31} is −3.29 dB. The simulated output phase difference at 6.5 GHz is 49.43° with a phase deviation of 4.43°. The rectangular ground slots are introduced in the proposed 3 dB/45° patch coupler 3 dB/45° patch coupler to enhance the bandwidth performances of S-parameters and output phase difference. As observed in Fig. 12(b), the −10 dB fractional bandwidths of S_{11} and S_{41} are 28.90% and 42.31% in simulation, whilst 37.08% and 46% in measurement. The respective −3 dB ± 1 dB bandwidths of S_{21} and S_{31} are 24.62% and 39.14% in simulation, whereas 42% and 37.08% in measurement. The bandwidth of 5° phase error is 35.91% in simulation, whereas 35.08% in measurement. At 6.5 GHz, the simulated S_{11} is −31.89 dB, whereas the simulated S_{41} is −38.55 dB. The measured S_{11} and S_{41} are −35 dB and −20.99 dB, respectively. The simulated S_{21} is −3.17 dB, whereas the measured S_{21} is −3.21 dB. Meanwhile, S_{31} is −3.28 dB in simulation, whereas −3.71 dB in measurement. The simulated output phase difference at 6.5 GHz is 45° without phase deviation, whereas the measured output

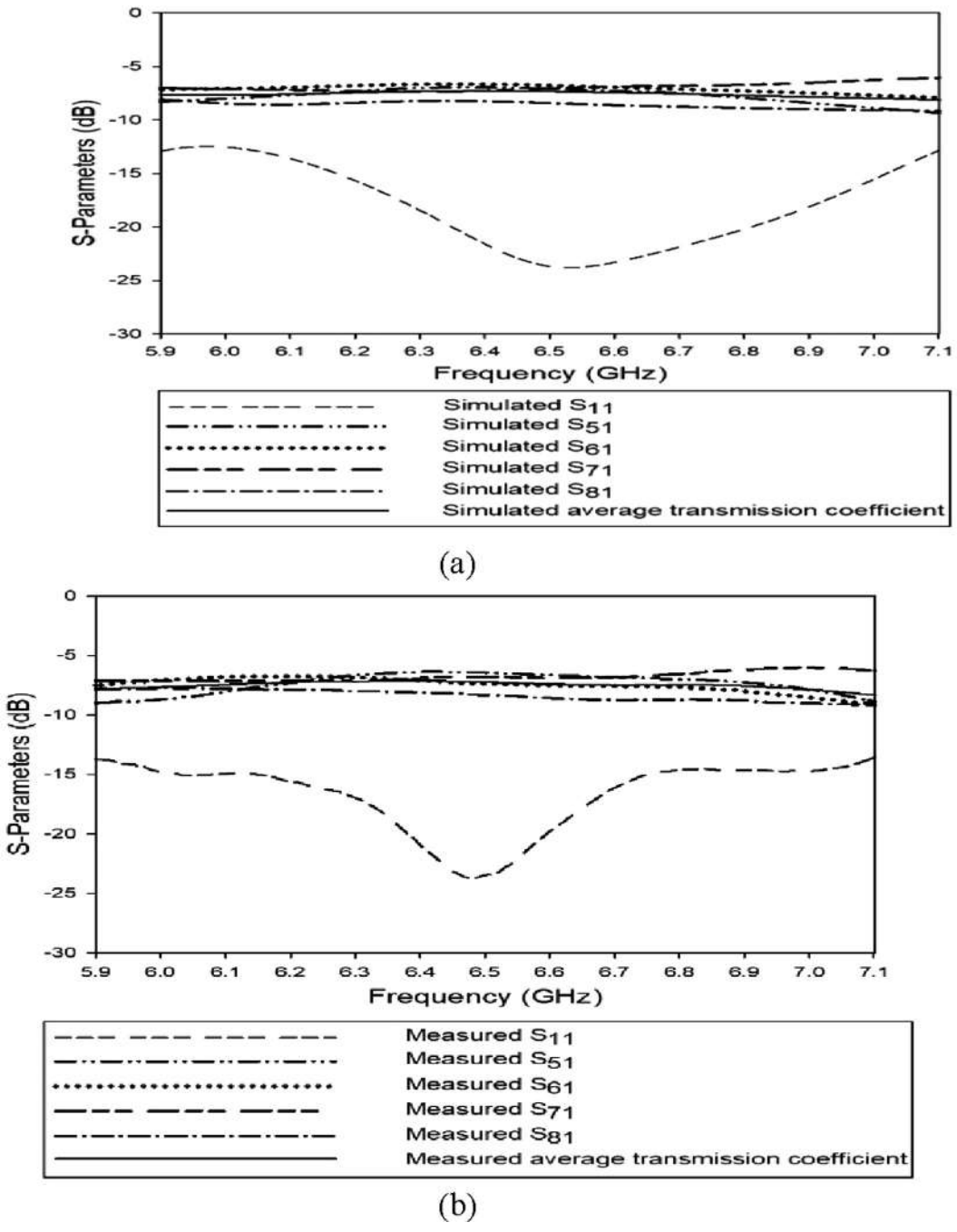

Fig. 14 S-parameter responses for the proposed 4 × 4 BM; (a) Simulation results (b) Measurement results.

phase difference is 46.62° with a phase deviation of ± 1.62°. Table 7 shows that the bandwidths of −10 dB S_{11}, 1 dB amplitude imbalance of S_{31} and 5° phase imbalance of output phase difference are enhanced due to the presence of rectangular ground slots at the bottom layer of the proposed 3 dB cross-slotted patch coupler. By doing this modification, the output phase difference of the proposed 3 dB/90° cross-slotted patch coupler is capable of reducing from 90° to 45° without interfering the performance of −3 dB coupling coefficient and maintaining the patch size. This coupler contributes a bandwidth enhancement of 15.84% compared to the integration of conventional 3 dB branch-line coupler and 45° Schiffman phase shifter. The size reduction and bandwidth improvement of the proposed 3 dB/45° patch coupler are achieved due to the elimination of 45° phase shifter from a combination of the traditional 3 dB branch-line coupler with 45° phase shifter.

3.3. Modified 0 dB/0° crossover

Fig. 13 depicts the simulation and measurement results of the modified 0 dB/0° crossover. At 6.5 GHz, the simulated S_{11}, S_{21}, S_{31} and S_{41} are −15.94 dB, −17.78 dB, −0.86 dB and −13.68 dB, respectively. Meanwhile, the S_{11}, S_{21}, S_{31} and S_{41} are –23.05 dB, −16.79 dB, −0.64 dB and −14.31 dB at

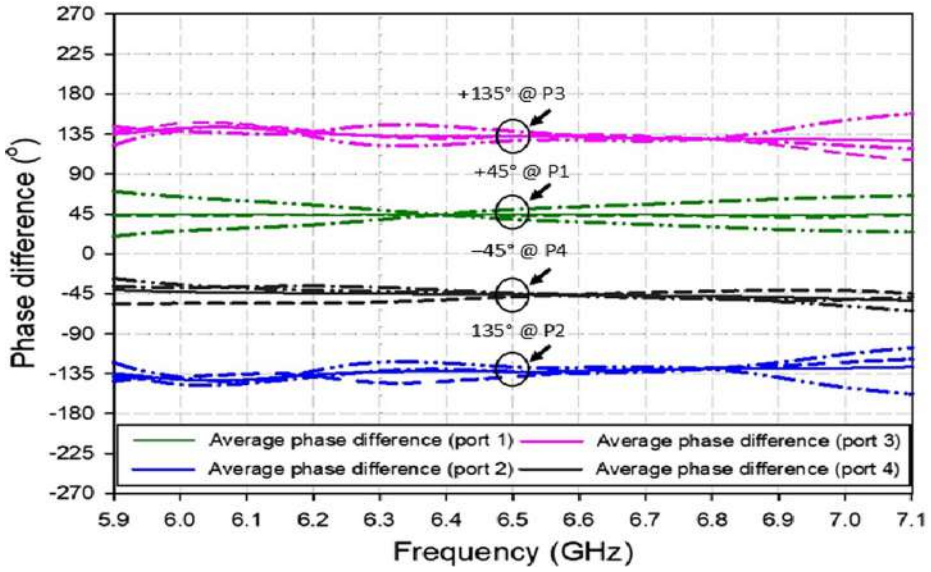

Fig. 15 Progressive phase differences of 4 × 4 BM when each port is driven.

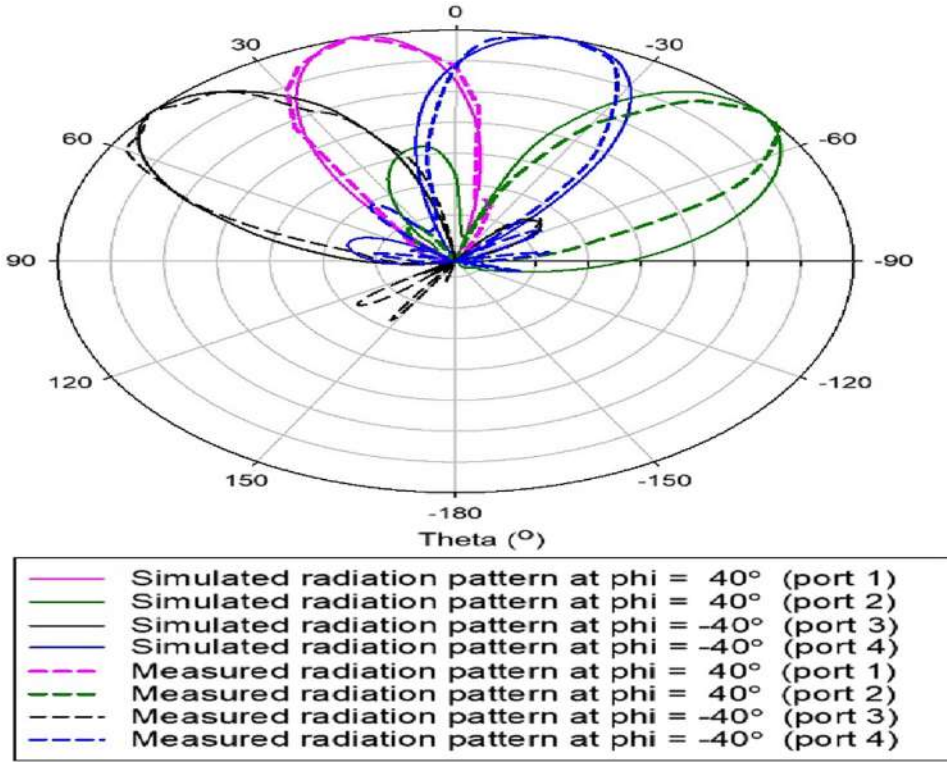

Fig. 16 Simulated and measured radiation patterns of the proposed 4 × 4 switched-beam BM for port 1 to port 4 excitations, respectively.

6.5 GHz. As observed, the simulated and measured output phase differences between output ports are 0.2° and 0.39° at 6.5 GHz, respectively.

3.4. Proposed 4 × 4 BM

The S-parameter responses and phase differences between consecutive output ports are only shown for signal excitation at input port 1 and port 2 due to the symmetrical nature of the BM device. Fig. 14 shows the simulation and measurement results of the S-parameter responses for the proposed 4 × 4 BM when port 1 is excited. The fractional bandwidth of −10 dB reflection coefficients is 18.46% in simulation and measurement. The bandwidth enhancement of −10 dB reflection coefficients for the proposed 4 × 4 BM is about 9.7% compared to the conventional 4 × 4 BM. The average of trans-

Table 6 Performance comparison between the 3 dB/90° cross-slotted patch coupler with the other patch coupler available in the recent literature.

References	[20]	This Work (Design B)
−10 dB bandwidth of S_{11} (%)	11.20	28
1 dB amplitude imbalance bandwidth of S_{31} (%)	10	36.46
5° phase imbalance bandwidth (%)	13.33	37.84
Electrical size ($\lambda_g \times \lambda_g$)	1.3 × 1.1	0.2 × 0.2

mission coefficients for all driven input ports are −6 ± 1.5 dB in both simulation and measurement at 6.5 GHz.

As observed, Fig. 15 shows the phase differences between consecutive output ports for the proposed 4 × 4 BM when each input port is excited. For example, the phase difference at port 1 excitation is calculated by the average of three values: ($\angle S_{51}$ - $\angle S_{61}$), ($\angle S_{61}$ - $\angle S_{71}$) and ($\angle S_{71}$ - $\angle S_{81}$). The output phase differences of +45°, –135°, +135° and –45° are achieved with a maximum average phase tolerance about ± 1.8° at 6.5 GHz in simulation and measurement when port 1 to port 4 are sequentially excited.

3.5. Proposed 4 × 4 switched-beam BM

The proposed 4 × 4 BM is further verified by integrating the inset feeding patch antenna to test the beam steering capability and obtain the radiation patterns. The simulated and measured radiation pattern results (normalized) of the proposed switched-beam 4 × 4 BM are depicted in Fig. 16. The simulated and measured beam directions are +15°, −50°, +50° and −15° when power is injected into port 1 to port 4, sequentially. The symmetric beam directions with opposite signs are observed when power is excited at port 3 or port 4 compared to the obtained beam directions by exciting port 1 or port 2 due to symmetric configuration of the proposed switched-beam 4 × 4 BM. The simulated and measured beam error is ± 0.58° compared to the theoretical calculation. The proposed switched-beam 4 × 4 BM exhibits a wide beam scanning angle between −50° and 50°. Input ports were driven sequentially while radiation patterns are simulated and measured at the best cutting angles in yz-plane. The maximum gain of the proposed switched-beam 4 × 4 BM is 9.84 dB.

4. Benchmarking with the contemporary state-of-the-art BM and switched-beam BM

Tables 8 and 9 present the results of numerous methodologies embraced by researchers for realizing 4 × 4 BMs and 4 × 4 switched-beam BMs, respectively. Parameters including the −10 dB fractional bandwidth S_{11}, amplitude imbalance of transmission coefficients, phase imbalance, relative area, size reduction from their conventional designs and maximum beam-steering are compared. The physical size of the proposed 4 × 4 BM and 4 × 4 switched-beam BM are reduced by 51.56% and 48.02% compared to its conventional BM. The proposed 4 × 4 BM shows a wide −10 dB fractional bandwidth S_{11} of 18.46% (5.9–7.1 GHz) and improved by 9.7%

Table 7 Performance comparison among the 3 dB/45° cross-slotted patch coupler without ground slot and with ground slots as well as other non-standard phase couplers.

References	[21]	[22]	[23]	3 dB/45° cross-slotted patch coupler	
				Without ground slots	With ground slots (proposed)
−10 dB bandwidth of S_{11} (%)	21.40	22	10	26.02	28.90
1 dB amplitude imbalance bandwidth of S_{31} (%)	24.50	42	30	33.90	39.14
5° phase imbalance bandwidth (%)	39.60	32	31	19.61	35.91
Electrical size ($\lambda_g \times \lambda_g$)	0.32 × 0.32	0.31 × 0.14	0.32 × 0.32	0.22 × 0.23	0.22 × 0.23

Table 8 Comparative study with the state-of-the-art 4 × 4 BM.

Performances	−10 dB fractional bandwidth S_{11}, (%)	Amplitude imbalance of transmission coefficients (dB)	Phase imbalance (°)	Relative area ($\lambda_0 \times \lambda_0$)	Size reduction from conventional design (%)
Conventional 4 × 4 BM	8.76	1.90	4.75	2.36 × 2.15	NA
[3]	0.80	1.69	0.52	3.10 × 2.33	NA
[24]	8.00	1.50	3.00	2.01 × 1.13	42.68
[25]	15.00	1.52	6.00	3.54 × 1.46	NA
[26]	14.49	1.56	10.00	3.03 × 3.03	NA
This work (Proposed 4 × 4 BM)	18.46	1.50	1.80	1.92 × 1.28	51.56

Table 9 Comparative study with the state-of-the-art 4 × 4 switched-beam BM.

References	Relative area ($\lambda_0 \times \lambda_0$)	Maximum beam-steering (°)
Conventional 4 × 4 switched-beam BM	2.36 × 2.77	45
[10]	3.21 × 3.20	47
[27]	2.17 × 1.77	38
[28]	2.80 × 1.20	29
[29]	2.79 × 2.98	40
This work (proposed 4 × 4 switched-beam BM)	1.92 × 1.77	50

compared to its conventional BM. This work has 1.5 dB amplitude imbalance of average transmission coefficient and 1.8° of average phase imbalance at 6.5 GHz. By comparing the performance results of the proposed 4 × 4 BM with the conventional BM and other related works, the proposed 4 × 4 BM exhibits the highest −10 dB fractional bandwidth and the lowest average amplitude imbalance of the transmission coefficients. The good trade-offs between size miniaturization and bandwidth enhancement are achieved. Additionally, the beam scanning angle (-50° to 50°) of the proposed 4 × 4 switched-beam BM is wider than its conventional BM and other related works. The comparative studies with state-of-the-art 4 × 4 BM and 4 × 4 switched-beam BM depicts the effectiveness of the proposed 4 × 4 BM and 4 × 4 switched-beam BM. Because the proposed 4 × 4 BM without phase shifter exhibits a compact size, wide impedance bandwidth, low-cost design and easy fabrication process, it will be an attractive candidate for the 5G communication system. This assessment confirms that the miniaturized 4 × 4 switched-beam BM without phase shifter ensures outstanding performance characteristics for 6 GHz band.

5. Conclusions

A miniaturized 4 × 4 BM without phase shifter has been designed and analyzed. The proposed 4 × 4 BM and 4 × 4 switched-beam BM contribute 51.56% and 48.02% of size reduction compared to their conventional designs. The proposed 4 × 4 BM exhibits a broad −10 dB impedance operation of 18.46% (5.9–7.1 GHz) and improved by 9.7% compared to the conventional BM that can cover the 6 GHz band of 5G spectrum. The low amplitude imbalances of the transmission coefficients (1.5 dB) and phase differences (1.8°) are accomplished at 6.5 GHz by the miniaturized 4 × 4 BM. Four switched-beams pointed at +15°, −50°, +50° and −15° are developed by the proposed 4 × 4 switched-beam BM with a wide beam scanning angle between −50° to 50°. The S-parameters, phase differences and radiation patterns demonstrate almost the same trend between simulated and measured results. The comparative studies with state-of-the-art 4 × 4 BM and 4 × 4 switched-beam BM depicts the effectiveness of the proposed 4 × 4 BM and 4 × 4 switched-beam BM. Because the proposed 4 × 4 switched-beam BM without phase shifter exhibits a compact size, wide impedance bandwidth, low-cost design and easy fabrication process, it will be an attractive candidate for the 5G communication system.

Declaration of Competing Interest

The authors declare that they have no known competing financial interests or personal relationships that could have appeared to influence the work reported in this paper.

Acknowledgments

This work is supported by Ministry of Higher Education, Malaysia under Fundamental Research Grant Scheme (203.PELECT.6071373).

References

[1] "Unlicensed Use of the 6 GHz Band, Notice of Proposed Rulemaking," Federal Communications Commission, Washington, D.C., 2020.
[2] H.N. Chu, T. Ma, An extended 4 x 4 Butler Matrix with enhanced beam controllability and widened spatial coverage, IEEE Trans. Microw. Theory Tech. 66 (3) (2018) 1301–1311.
[3] V. Prakash et al, Design of 4 x 4 Butler Matrix and its process modeling using petri nets for phase array systems, Prog. Electromagn. Res. C (PIER C). 103 (2020) 137–153.
[4] Y. Yang, Y.F. Pan, S.Y. Zheng, W. Hong, W.S. Chan, Analytical design method and implementation of broadband 4 × 4 Nolen matrix, IEEE Trans. Microw. Theory Tech. 70 (1) (2022) 343–355.
[5] P. Li, H. Ren, B. Arigong, A symmetric beam-phased array fed by a Nolen matrix using 180° couplers, IEEE Microwave Wirel. Compon. Lett. 30 (4) (2020) 387–390.
[6] C. Tsokos et al, Analysis of a multibeam optical beamforming network based on Blass matrix architecture, J. Lightwave Technol. 36 (16) (2018) 3354–3372.
[7] D.I. Lialios, C.L. Zekios, S.V. Georgakopoulos, Design of a mm-Wave Double-Sided Substrate Blass Matrix Beamforming Network, in: 2021 IEEE 21st Annual Wireless and Microwave Technology Conference (WAMICON), 2021, pp. 1–4.
[8] Y. Liu, H. Yang, Z. Jin, F. Zhao, J. Zhu, A multibeam cylindrically conformal slot array antenna based on a modified Rotman lens, IEEE Trans. Antennas Propag. 66 (7) (2018) 3441–3452.
[9] M.R. Nikkhah, M. Hiranandani, A.A. Kishk, Rotman lens design with wideband DRA array, Prog. Chem. Org. Nat. Prod. In Electromagnetics Research. 169 (2020) 45–57.
[10] Y. Wang, K. Ma, Z. Jian, A low-loss Butler Matrix using patch element and honeycomb concept on SISL platform, IEEE Trans. Microw. Theory Tech. 66 (8) (2018) 3622–3631.
[11] A.M. Zaidi, B.K. Kanaujia, M.T. Beg, J. Kishor, K. Rambabu, A novel dual-band branch line coupler for dual-band Butler Matrix, IEEE Trans. Circuits Syst. II Express Briefs 66 (12) (2019) 1987–1991.
[12] Z. Mousavi, P. Rezaei, Millimetre-wave beam-steering array antenna by emphasising on improvement of Butler Matrix features, IET Microwaves Antennas Propag. 13 (9) (2019) 1287–1292.
[13] A. Tajik, A. Shafiei Alavijeh, M. Fakharzadeh, Asymmetrical 4 × 4 Butler Matrix and its application for single layer 8 × 8 Butler Matrix, IEEE Trans. Antennas Propag. 67 (8) (2019) 5372–5379.
[14] E.T. Der, T.R. Jones, M. Daneshmand, Miniaturized 4 × 4 Butler Matrix and tunable phase shifter using ridged half-mode substrate integrated waveguide, IEEE Trans. Microw. Theory Tech. 68 (8) (2020) 3379–3388.
[15] L.M. Zheng, Z.T. Lu, B.W. Xu, S.Y. Zheng, Flexible millimeter-wave Butler Matrix based on the low-loss substrate integrated suspended line patch hybrid coupler with arbitrary phase

difference and coupling coefficient, Int. J. Rf Microwave Comput.-aided Eng. (2021) 1–14.
[16] N. Jizat, Z. Yusoff, Y. Yamada, N. Zainudin, Design of via-hole for dual layer Butler Matrix, in: 2019 IEEE Asia-Pacific Conference on Applied Electromagnetics (APACE), 2019, pp. 1–5.
[17] J. Park, J. Kim, A 28 GHz CMOS Butler Matrix for 5G mm-wave beamforming systems, Microwave Opt. Technol. Lett. (2020) 1–7.
[18] Q.P. Chen, Z. Qamar, S.Y. Zheng, Y. Long, D. Ho, Design of a compact wideband Butler Matrix using vertically installed planar structure, IEEE Trans. Compon. Packag. Manuf. Technol. 8 (8) (2018) 1420–1430.
[19] M. Chowdhury, A. Biswas, Wireless Communication: Theory and Applications, first ed., Cambridge University Press, India, Cambridge, 2017.
[20] X.F. Ye, S.Y. Zheng, Y.M. Pan, A compact millimeter-wave patch quadrature coupler with a wide range of coupling coefficients, IEEE Microwave Wirel. Compon. Lett. 26 (3) (2016) 165–167.
[21] A. Singh, M.K. Mandal, Arbitrary coupling arbitrary phase couplers with improved bandwidth, IET Microwaves Antennas Propag. 13 (6) (2019) 748–755.
[22] Y. Wu, L. Jiao, Q. Xue, et al, A universal approach for designing an unequal branch-line coupler with arbitrary phase differences and input/output impedances, IEEE Trans. Compon. Packag. Manuf. Technol. 7 (6) (2017) 944–955.
[23] Q. He, C. Qi, C. Liu, et al, A compact arbitrary power division coupler with nonstandard phase-difference, J. Electromagn. Waves Appl. 32 (3) (2017) 293–305.
[24] P. Bhowmik, T. Moyra, Modelling and validation of a compact planar Butler Matrix by removing crossover, Wireless Personal Commun.: Int. J. 95 (4) (2017) 5121–5132.
[25] H. Ren, B. Arigong, M. Zhou, J. Ding, H. Zhang, A novel design of 4 × 4 Butler Matrix with relatively flexible phase differences, IEEE Antennas Wirel. Propag. Lett. 15 (2016) 1277–1280.
[26] K. Bharath et al, Millimeter wave switched beam rectangular loop dipole antenna array using a 4 × 4 Butler Matrix, Progress Electromagn. Res. C. 117 (2021) 251–260.
[27] Y. Kim, Y. Kim, H. Dong, Y.S. Cho, H.L. Lee, Compact switched-beam array antenna with a Butler Matrix and a folded ground structure, Electronics 9 (2) (2020) 1–12.
[28] N.M. Jizat, N. Ahmad, Z. Yusoff, N.M. Nor, M.I. Sabran, 5G beam-steering 2 × 2 Butler Matrix with slotted waveguide antenna array, Telkomnika 17 (4) (2019) 1656–1662.
[29] S. Trinh-Van, J.M. Lee, Y. Yang, K.Y. Lee, K.C. Hwang, A sidelobe-reduced, four-beam array antenna fed by a modified 4 × 4 Butler Matrix for 5G applications, IEEE Trans. Antennas Propag. 67 (7) (2019) 4528–4536.